DOI: 10.61782/fa.2023.0431

forum acusticum 2023

On the bifurcations of a fluttering plate in confined axial flow

Filipe Soares[1*] **Christophe Vergez**[2] **Jose Antunes**[1]
Vincent Debut[3] **Bruno Cochelin**[2] **Fabrice Silva**[2]

[1] Instituto Superior Técnico – C2TN, Lisbon, Portugal
[2] Aix-Marseille Université, CNRS, Centrale Marseille, LMA UMR7031, Marseille, France
[3] Instituto Politécnico de Castelo Branco – ESAA, Castelo Branco, Portugal

ABSTRACT

The flutter of cantilevered beams in channel flow is a benchmark example of flow-induced vibrations and its fundamental behavior is found in numerous practical applications. Experiments have shown that such systems present a wide variety of complex nonlinear behavior. However, the plethora of previous studies is mostly concerned with linear stability analysis. In this work, we provide an initial impulse for a comprehensive nonlinear study of these systems through bifurcation analysis. We consider a one-dimensional problem, where a cantilevered beam is treated in a modal framework and the surrounding flow is modelled by bulk-flow equations. The system is discretized in space and time via Galerkin procedures (modal, Tau and harmonic balance methods) and the continuation of periodic solutions is pursued using the asymptotic numerical method. The nonlinear dynamics are explored with respect to various dimensionless parameters, clarifying a number of behavioral trends: sub-critical bifurcations and hysteresis loops, grazing boundaries (separation between limit cycles with and without intermittent beam-wall impacts), internal resonances, torus bifurcations and quasi-periodic oscillations, amongst others. Aside from providing novel insights into the physics of fluttering beams, is it hoped that the methods used in here can stimulate similar studies in the field of flow-induced vibrations.

Keywords: *Flow-induced vibration, plates in axial flow, bifurcation analysis, hysteresis.*

[*] ***Corresponding author**: filipedcsoares@gmail.com*

1. MODEL DESCRIPTION

The considered model describes the FSI of a cantilevered beam in channel flow as shown in Figure 1.

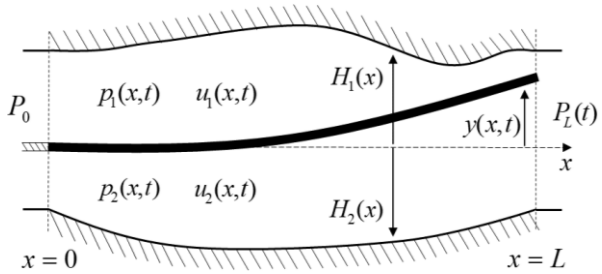

Figure 1. Diagram of the 1D model.

The dynamics of the linear cantilevered beam are defined in a modal framework. The vertical displacement of the beam $y(x,t)$ is developed as

$$y(x,t) = \sum_{m=1}^{M} \varphi_m(x) q_m(t) \quad (1)$$

where $q_m(t)$ and $\varphi_m(x)$ are the modal displacements and shapes, respectively. The dynamics of the beam are given, as usual, by a set of M modal equations

$$\ddot{q}_m(t) + 2\omega_m \zeta_m \dot{q}_m(t) + \omega_m^2 q_m(t) = F_m(t) \big/ m_m \quad (2)$$

where m_m, ω_m, ζ_m and $F_m(t)$ are the masses, frequencies, damping ratios and external forces. The external modal forces $F_m(t)$ are then given by the projection of the flow pressure fields on the upper and lower sides of the beam, $p_1(x,t)$ and $p_2(x,t)$, unto the modal basis

$$F_m(t) = M^* \int_0^1 [p_2(x,t) - p_1(x,t)] \varphi_m(x) dx \quad (3)$$

where the fluid-beam mass ratio is written explicitly as $M^* = \rho L / \rho_s e$; ρ is the density of the fluid and e denotes the thickness of the beam.
Assuming incompressible and inviscid flow, the momentum and continuity equations for the flow in each channel c are given in dimensionless form by

$$\frac{\partial u_c}{\partial t} + u_c \frac{\partial u_c}{\partial x} + \frac{\partial p_c}{\partial x} = 0 \quad (4)$$

$$\frac{\partial h_c}{\partial t} + \frac{\partial}{\partial x}(h_c u_c) = 0 \quad (5)$$

Following previous work [4], localized dissipative effects are enforced at the boundary conditions at $x = 0$ and $x = 1$:

$$p_c(0,t) = P_0(t) - \frac{1}{2}\left[u_c(0,t)\right]^2 - \frac{1}{2}\left|u_c(0,t)\right| u_c(0,t) K_0$$
$$p_c(1,t) = P_L(t) - \frac{1}{2}\left[u_c(1,t)\right]^2 + \frac{1}{2}\left|u_c(1,t)\right| u_c(1,t) K_L \quad (6)$$

where K_0 and K_L are the entry and exit head-loss coefficients, while $P_0(t)$ and $P_L(t)$ are pressure imposed at the entry and exit of the domain.

2. SPATIAL & TEMPORAL DISCRETIZATION

For compactness, here we restrain from showing the details of the spatial discretization procedure used here to convert the PDE system (4)-(6) into a set of time-dependent equations (ODE/DAE system). The interested reader is referred to the authors previous work [6]. Essentially, the pressure and velocity fields in each channel are developed in terms of a set of orthogonal basis functions

$$u_c(x,t) = \sum_{n=0}^{N} T_n(x) u_n(t); \quad p_c(x,t) = \sum_{r=0}^{N} T_r(x) p_r(t) \quad (7)$$

where $T_n(x)$ are Chebyshev polynomials of the first kind. After a modified Galerkin projection (Tau-method) on the fluid equations of each channel $c = 1, 2$, and assembly with the structural equations (2), the resulting coupled system is a system of first-order nonlinear differential-algebraic equations (DAE) of size $2M + 4(N+1)$ and differential index-2.
Contrary to previously derived formulations [5] the Galerkin approach presented here allows us to discretize the continuous 1-D problem into a set of nonlinear time-dependent equations, compatible for use in algorithms for the continuation of periodic solutions. In this work we have used the open-source software Manlab 4.0 [7] which combines the Harmonic Balance Method (HBM) for the time-discretization with the Asymptotic Numerical Method (ANM) for the numerical continuation of the solution path.

3. ILLUSTRATIVE RESULTS

The linear stability analysis of the system is often the primary information to extract [1-3]. A typical result is shown in Figure 2-(a), where the stability boundaries of the equilibrium solution in the $M^* - U^*$ plane are shown for a symmetric configuration with constant channel heights and fixed confinement ratio $H^* = 0.1$ and structural damping $\zeta_n = 0.5\%$.

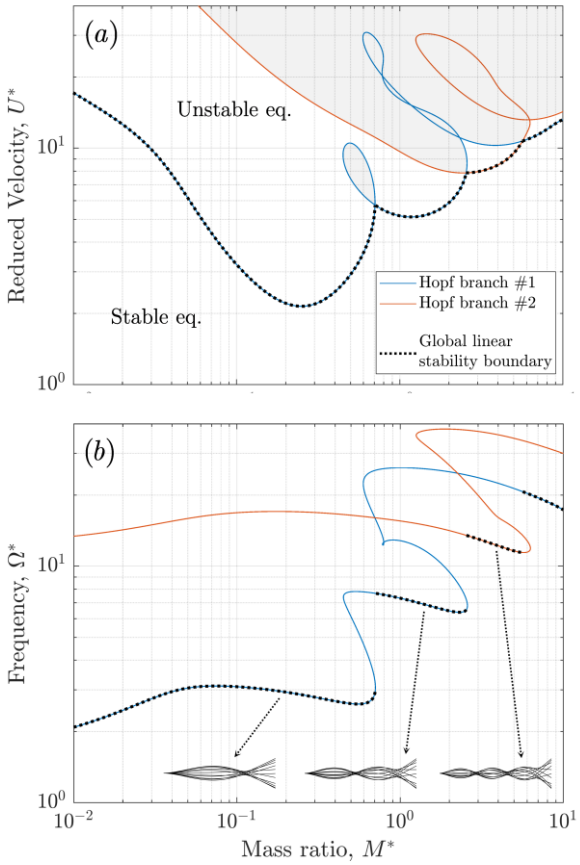

Figure 2. Linear stability map for a system with constant symmetric channels: (a) Hopf bifurcation branches and global linear stability boundary in the $M^* - U^*$ plane; (b) corresponding critical frequencies $\Omega^* = \omega^* / \omega_0$.

We notice there are two Hopf bifurcation branches whose combination forms a global linear stability boundary, i.e.

the typical "cascading" frontier commonly found in literature [5,11]. In this boundary, each step in the "cascade" corresponds to a change of shape of the primary unstable mode, as illustrated in the bottom of Figure 2-(b).

3.1 Constrained continuation and an "augmented" linear stability analysis

Although undeniably useful, linear stability analysis is, by default, unable to characterize the sub- or super-critical nature of the Hopf bifurcations (HB), a widely discussed and ill-explained phenomena that could explain the hysteresis loops commonly reported in experiments. Nevertheless, here we propose a method to calculate an "augmented" linear stability analysis. The general idea is to add a constraint equation that fixes the amplitude of oscillation of a particular limit-cycle to a small value ε

$$y_L(t=0) = \sum_{h=1}^{H} a_h = \varepsilon \qquad (8)$$

where y_L is the beam-tip displacement, a_h are the coefficients of the harmonic balance expansion and H is the harmonic truncation. Effectively, this additional constraint allows us to follow branches of periodic solutions that are arbitrarily close to the Hopf bifurcation branch. More importantly however, we are then able to access their stability and hence distinguish between super-critical and sub-critical bifurcations. To illustrate, linear stability boundaries are shown in Figure 3 for a symmetric system with two modes $M = 2$, $H^* = 0.1$ and different values of structural damping ζ_n.

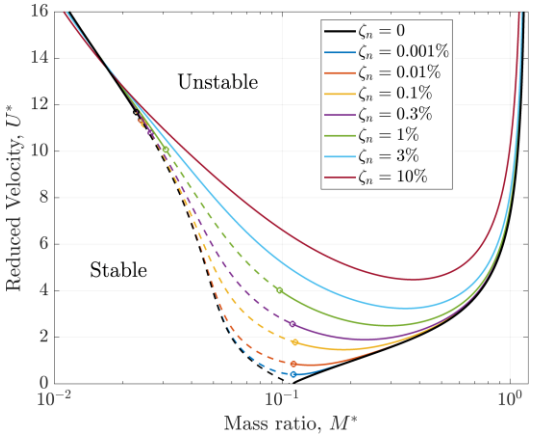

Figure 3. Effect of structural damping ζ_n on the Hopf bifurcations branches for a symmetric system in inviscid flow. Solid and dotted lines represent super- and sub-critical bifurcations, respectively, while the circles denote Bautin bifurcations.

3.2 Nonlinear analysis of hysteresis

It is worth noting that hysteretic behavior is not unique to sub-critical Hopf bifurcations, and it can also appear in super-critical ones, via a double-fold bifurcation loop. To clarify the nature of this behaviour, several branches of periodic solutions were calculated for the same parameter configuration as above. Figure 4 illustrates a three-dimensional bifurcation diagram where multiple solution branches (at constant M^*) are shown around the region where hysteresis is predicted.

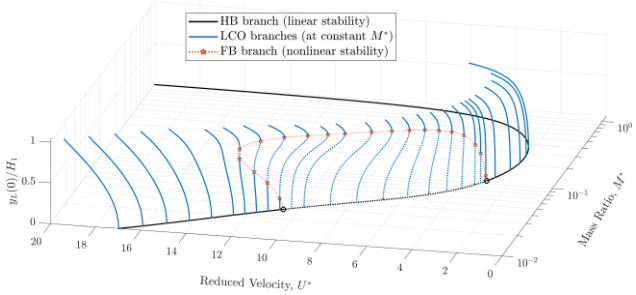

Figure 4. Three-dimensional view of the branches of periodic solutions (at constant M^*) stemming from the HB boundary.

From Figure 4 it becomes clear that such systems can encounter both super-critical and sub-critical bifurcations, depending on the specific parametric configuration. Notably, we observe that the two Bautin points (codimension-2 bifurcations) along the Hopf branches are actually the birthing points of a fold-bifurcation (FB) branch. This FB branch travels the surface defined by the periodic solution and outlines a frontier separating stable from unstable periodic solutions. The analysis of this type of FB branch, and how it varies depending on different parameters of the system, is of paramount importance to understand and quantify the hysteresis phenomena. Even though in this work we do not conduct a detailed parametric analysis, the presented results serve as an example of potential avenues of research in the analysis of fluttering beams but also, more generally, in the field of flow-induced vibrations, where hysteresis occurs frequently in various contexts.

3.3 Rich nonlinear behavior in systems with several beam modes

When considering a system with several beam modes, more complex nonlinear behavior is observed. These include: internal resonances, zones with multiple periodic solutions as well as torus bifurcations and associated quasi-periodic

motions. To illustrate some of the encountered dynamics, Figure 5 shows the bifurcation diagram in terms of the reduced velocity U^* for a symmetric system with 10 beam modes, $H^* = 0.1$, $\zeta_n = 0.5\%$ and $M^* = 0.5$.

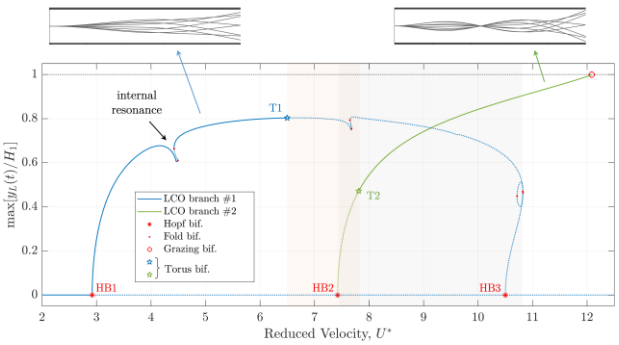

Figure 5. Bifurcation diagram at constant mass-ratio $M^* = 0.5$, illustrating the two branches of periodic solutions with respect to the reduced velocity U^*. The notation HB and T denote Hopf and torus bifurcations respectively. The orange area indicates that no stable periodic solution exists while the grey area indicates regions where multiple oscillatory solutions co-exist.

Figure 5 shows the bifurcation diagram at mass-ratios close to a "step-transition" in the cascading linear boundary (see Figure 2), and illustrates the array of different nonlinear phenomena describe above. Once the equilibrium becomes unstable (HB1) a branch of periodic solutions associated with "single-neck" beam motions emerges. This branch then encounters a fold-loop associated with an internal resonance (when the frequency of oscillation becomes is close to an integer multiple of another beam mode – in this case $\Omega_0 \approx 3\omega_3$). At $U^* \approx 6.5$, this branch loses its stability through a torus bifurcation (T1). In the succeeding orange area, quasi-periodic motions arise since no stable periodic nor equilibrium solutions exist. Further on, a second Hopf bifurcation (HB2) gives rise to another branch of periodic solutions associated with "double-neck" beam motions. Contrary to the first branch, this one is initially unstable and then stabilizes through a torus bifurcation (T2), before it encounters a grazing boundary (where impacts between the beam and the side-walls become inevitable. Aside from showcasing various nonlinear phenomena associated with this type of systems, this example also illustrates potential ways in which a "mode-transition" (between single- and double-neck solutions) can occur.

4. CONCLUSION

The nonlinear dynamics of a cantilever beam in confined axial flow were studied using continuation methods. Contrary to previous nonlinear studies, reliant on time-domain integrations, the bifurcation analysis presented here provides a more complete overview of the dynamics found in this type of systems. Notably, the ill-explained phenomena of hysteresis, commonly observed in experiments, was discussed. Results suggest that flutter instabilities can be a product of both super- or sub-critical Hopf bifurcations, depending on different system parameters. Additionally, a method for the continuation of Hopf bifurcation branches, which distinguishes their sub/super-critical nature was proposed. Numerical results also display a wide variety of nonlinear dynamical behavior including internal resonances, zones of multi-stability, torus bifurcations and quasi-periodic solutions. Aside from providing novel insights into the physics of fluttering beams and suggesting news avenues of research, is it hoped that the methods and results presented here can stimulate similar studies in the field of flow-induced vibrations.

5. REFERENCES

[1] M. P. Paidoussis, Fluid-Structure Interactions: Slender Structures and Axial Flow, San Diego, California: Academic Press, 2004.

[2] Y. Yu, Y. Liu and X. Amandolese, "A Review on Fluid-Induced Flag Vibrations," *Applied Mechanics Reviews,* vol. 71, no. 010801, 2019.

[3] K. Shoele and R. Mittal, "Flutter instability of a thin flexible plate in a channel," *Journal of Fluid Mechanics,* vol. 786, pp. 29-46, 2016.

[4] X. Wu and S. Kaneko, "Linear and Nonlinear analyses of sheet flutter induced by leakage flow," *Journal of Fluids and Structures,* vol. 20, pp. 927-948, 2005.

[5] F. Soares, J. Antunes, V. Debut, C. Vergez, B. Cochelin and F. Silva, "A nonlinear analytical formulation for the 1D modelling of a flexible beam in channel flow," *Journal of Fluids and Structures,* vol. 113, 2022.

[6] F. Soares, J. Antunes, V. Debut, C. Vergez, B. Cochelin and F. Silva, "A Galerkin formulation for the nonlinear analysis of a flexible beam in channel flow," *Journal of Fluids and Structures*, 2023.

[7] "Manlab: An interactive path-following and bifurcation analysis software," [Online]. Available: http://manlab.lma.cnrs-mrs.fr/. [Accessed 23 November 2022].

[8] C. Eloy, R. Lagrange, C. Souilliez and L. Schouveiler, "Aeroelastic instability of cantilevered flexible plates in uniform flow," *Journal of Fluid Mechanics,* vol. 611, pp. 97-106, 2008.